Quantum Electronics **50** (4) 386–391 (2020)

https://doi.org/10.1070/QEL17267

Numerical simulation of dispersion and nonlinear characteristics of microstructured silica fibres with a thin suspended core in a wide range of their parameters

E.A. Anashkina, A.V. Andrianov, G. Leuchs

Abstract. **Dispersion and nonlinear characteristics of microstructured silica fibres with a thin suspended core surrounded by three, four or six air holes have been studied theoretically in the wavelength range 1–2 μm. It has been shown that, owing to strong fundamental mode confinement near the core, the Kerr nonlinearity coefficient can exceed the nonlinearity coefficient of standard telecom fibre SMF28e by two orders of magnitude. The large waveguide contribution allows for effective group velocity dispersion management. Estimates are presented that demonstrate the feasibility of using suspended core fibre exhibiting Kerr nonlinearity for generating non-classical light: a state with squeezed quantum fluctuations in one of the quadrature components of a cw laser signal at a wavelength near 1.55 μm.**

Keywords: *microstructured fibre, Kerr nonlinearity, group velocity dispersion.*

1. Introduction

In designing waveguide structures, considerable attention is paid to the refractive index profile, because most important characteristics depend on it. Modern technologies enable one to tune dispersion and nonlinear properties of waveguide structures in a wide range by producing specialty refractive index profiles. Microstructuring is widely used to control group velocity dispersion (GVD): one produces ordered structures of air holes or glasses differing considerably in refractive index, with characteristic sizes at a micron or submicron level [1–8]. In addition to widespread photonic crystal fibre, whose core is surrounded by several regular rings of air holes [3], there is suspended core fibre (SCF), in which a thin core is surrounded by one ring of air holes separated by thin walls [9–15]. Microstructured waveguide structures are often used to produce anomalous dispersion at wavelengths corresponding to normal material dispersion. A large waveguide contribution can considerably shift the zero dispersion wavelength. It is also possible to produce optical fibre with two (or three) GVD zeros in a particular spectral range [16]. Microstructured fibres with controlled dispersion and strong Kerr nonlinearity considerably extend the possibilities of nonlinear optical signal conversion; make it possible to obtain unique characteristics of light, unattainable for lasing, to master spectral ranges where no gain media are available [3, 5, 11] and to produce a supercontinuum – an ultrabroadband coherent signal with a spectral width of the order of an octave or even more [3, 11]; and can be used as nonlinear elements in measurements of the shape and phase of ultrashort pulses [15]. In addition to the above-mentioned classical nonlinear optical effects in microstructured fibre, one can observe quantum effects (see e.g. Refs [17–19]), but these have been the subject of much less extensive studies.

In this paper, we present numerical simulation of nonlinear and dispersion characteristics of SCF in a wide range of its parameters. These characteristics strongly depend on the geometric dimensions of structural elements of the fibre. Such fibre can be used in a wide range of above-mentioned classical nonlinear optical problems. In addition, we assess the feasibility of using the fibre under study, with adequately chosen parameters, for producing a non-classical state of light with squeezed quantum noise (squeezed quantum fluctuations in one of the signal quadrature components [20]). In some problems, e.g. in precision metrology (including laser interferometer gravitational wave detection), there is special interest in the ability to suppress noise to below the standard quantum limit, i.e. to generate so-called squeezed light.

Since the first observation of squeezed light by Slusher et al. [21], higher and higher degrees of quantum squeezing have been being reported [22]. The record high value (–15 dB) [23] was achieved under ideal conditions for cw radiation in the vacuum state – a so-called squeezed vacuum state of light. It is possible to squeeze quantum uncertainty using Kerr nonlinearity, which was demonstrated e.g. by Milburn et al. [24]. In this case, quantum uncertainty squeezing occurs for a quadrature inclined at some angle in phase space, and it cannot be directly measured via simple direct detection (but the problem can be obviated e.g. using a phase-shifting cavity). Previously, using telecom components and Kerr nonlinearity in fibre, Bergman and Haus [25] investigated noise reduction in the case of pulsed laser light. They achieved quantum squeezing in a nonlinear interferometer. In this process, the squeezed Wigner distribution rotated in phase space through a required angle, at which the squeezed quadrature could be measured by a simple method [26]. Squeezing was brought about for soliton pulses in a Sagnac interferometer fabricated from standard optical telecom fibre. A nonlinear fibre interferometer was also used to reduce classical noise by 12 dB [27] without reaching a level below quantum noise.

E.A. Anashkina, A.V. Andrianov, G. Leuchs Institute of Applied Physics, Russian Academy of Sciences, ul. Ulyanova 46, 603950 Nizhny Novgorod, Russia;
e-mail: elena.anashkina@gmail.com

Received 4 February 2020
Kvantovaya Elektronika **50** (4) 386–391 (2020)
Translated by O.M. Tsarev

Note that, for quantum squeezing of light in fibre, use is commonly made of all-solid silica fibre [25, 28], but photonic crystal fibre also can be used [19, 29]. Owing to the decrease in mode diameter, fibre microstructuring ensures higher nonlinearity in comparison with standard telecom fibre [3] and dispersion management, which is important in dealing with soliton pulses. In this paper, we demonstrate that the nonlinearity coefficient of fibre having a micron-sized suspended core can be several tens of times that of standard fibre, which is a favourable factor for studying nonlinear-optical and quantum effects.

2. Numerical simulation of dispersion and Kerr nonlinearity coefficients

SCF can be fabricated via precision drilling of holes around its core in a monolithic cylindrical glass preform, followed by fibre drawing at a controlled gas pressure in the holes. SCFs can have different numbers of air holes [9, 11–15]. We studied in detail SCFs having three, four and six air holes: SCF3, SCF4 and SCF6, respectively. Their cross sections are shown in Fig. 1 (top row). The core size was taken to be the diameter d of the inscribed circle. In simulating properties of the SCFs, described in terms of Maxwell's equations [30], we employed the finite element method. Using it, we found the propagation constant β and field structure of the fibre fundamental modes, which allowed us to calculate the second-order dispersion coefficient $\beta_2 = \partial^2\beta/\partial\omega^2$ and Kerr nonlinearity coefficient γ as functions of wavelength λ ($\lambda = 2\pi c/\omega$, where ω is the angular frequency and c is the speed of light) [16]. For comparison and qualitative understanding of the general relationships involved, we examined an axisymmetric core in air (SCF0) as well. In the case of SCF0, to verify the results obtained by the finite element method, we solved the problem using a simpler approach as well, in the axisymmetric core approximation. For an axisymmetric core, the characteristic equation derived for fundamental modes from Maxwell's equations and the continuity condition for tangential field components can be written in the form [30]

$$\left[\frac{J_1'(U)}{UJ_1(U)} + \frac{K_1'(W)}{WK_1(W)}\right]\left[\frac{J_1'(U)}{UJ_1(U)} + \left(\frac{1}{n}\right)^2 \frac{K_1'(W)}{WK_1(W)}\right] = \left(\frac{1}{U^2} + \frac{1}{W^2}\right)\left[\frac{1}{U^2} + \left(\frac{1}{n}\right)^2 \frac{1}{W^2}\right], \quad (1)$$

$$U = a\sqrt{k_0^2 n^2 - \beta^2}, \qquad W = a\sqrt{\beta^2 - k_0^2},$$

where J_1 is the first-order Bessel function of the first kind; K_1 is the first-order modified Bessel function of the second kind (Macdonald function); primes denote differentiation of a function with respect to its argument; a is the core radius ($a = d/2$); $k_0 = \omega/c$; and n is the refractive index. In this study, the refractive index was determined using the Sellmeier equation for fused silica [16]:

$$n^2(\omega) = 1 + \sum_{j=1}^{3} \frac{B_j \omega_j^2}{\omega_j^2 - \omega^2}, \quad (2)$$

where $B_1 = 0.6961633$; $B_2 = 0.4079426$; $B_3 = 0.8974794$; $\lambda_1 = 0.0684043$ μm; $\lambda_2 = 0.1162414$ μm; $\lambda_3 = 9.896161$ μm; and $\lambda_j = 2\pi c/\omega_j$.

After substitution of (2), the transcendental equation (1) was solved numerically by a modified Newton method. The results obtained by solving the characteristic equation (1) and by the finite element method for SCF0 were found to be in excellent agreement. The analytical expressions for the electric and magnetic fields are rather cumbersome [30], so we do not present them here.

The Kerr nonlinearity coefficient was calculated as follows:

$$\gamma = \frac{2\pi}{\lambda} \frac{\int n_2 P_z^2 \, \mathrm{d}^2 r}{\left(\int P_z \, \mathrm{d}^2 r\right)^2}, \quad (3)$$

where P_z is the z-axis projection of the Poynting vector; n_2 is the nonlinear refractive index of the glass ($n_2 = 2.6 \times 10^{-16}$ cm^2 W^{-1});

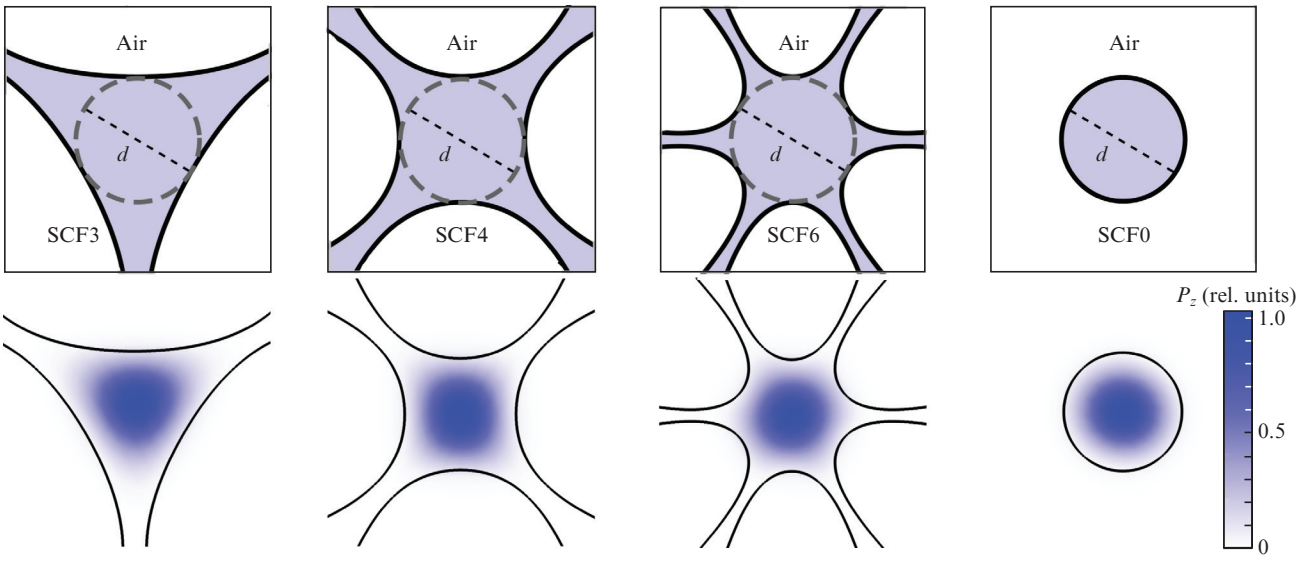

Figure 1. Cross sections of the microstructured suspended core fibres under consideration (top row) and Poynting vector projections calculated for the fundamental modes at a wavelength of 1.55 μm for fibres with $d = 2$ μm (bottom row).

and d^2r is a cross-sectional area element of the SCF. The calculated Poynting vectors at a wavelength of 1.55 μm for the fibres width $d = 2$ μm are shown in the bottom row in Fig. 1.

Figure 2 shows the calculated group velocity dispersion and Kerr nonlinearity coefficient as functions of wavelength in the range 1–2 μm for all the geometries under consideration. The calculated characteristics of the SCF3, SCF4 and SCF6 fibres differ only slightly. The SCF0 fibres differ from them more significantly because of the larger waveguide contribution. The calculated dispersion and nonlinearity coefficients of SCF6 differ least from those of SCF0, which is easy to explain: the larger the number of air holes around a core, the more similar is its cross section to a circle. For all geometries, the large waveguide contribution strongly shifts the zero

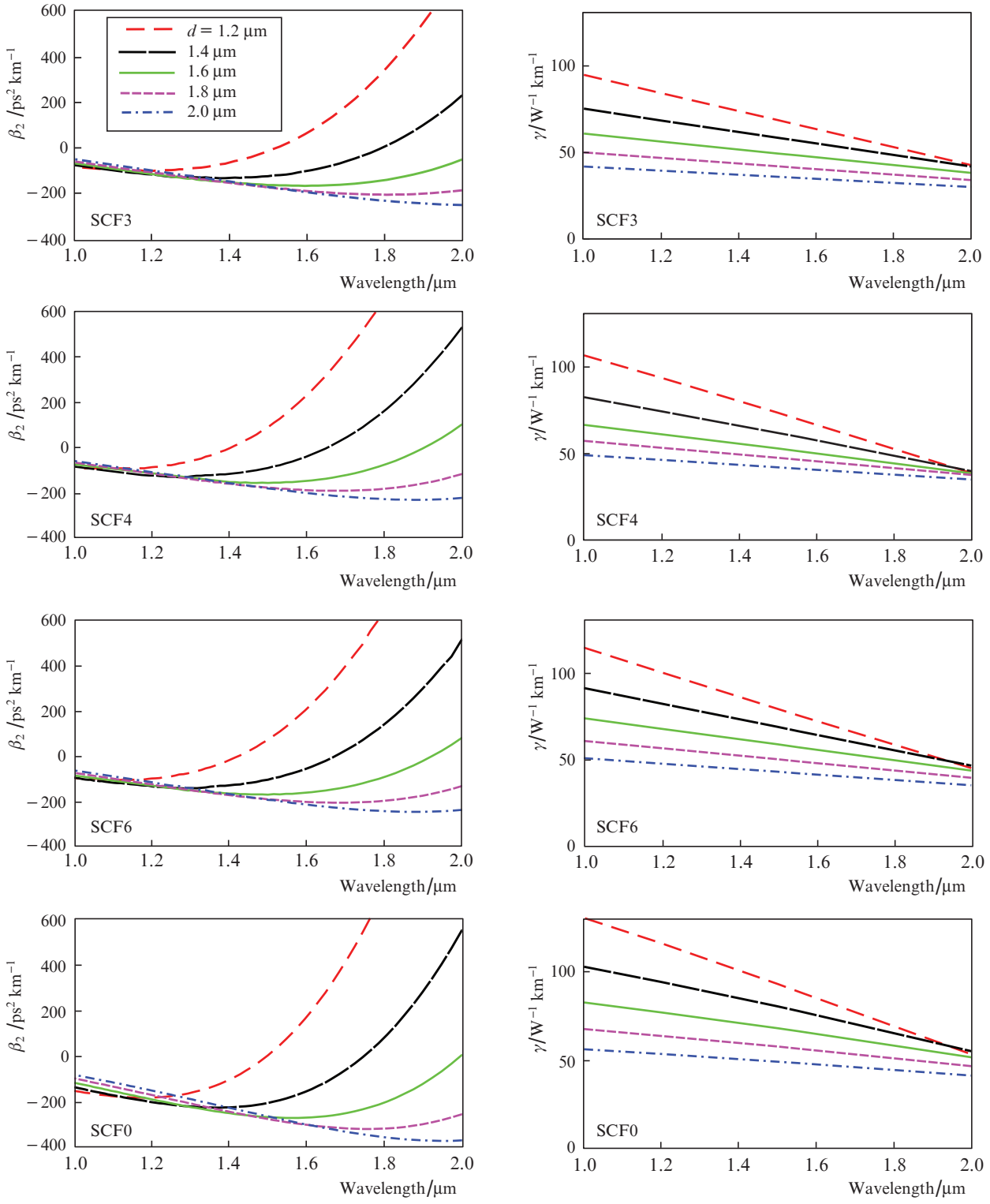

Figure 2. Group velocity dispersion and Kerr nonlinearity coefficient as functions of wavelength for SCF3, SCF4, SCF6 and SCF0, differing in core diameter.

dispersion wavelength relative to the material dispersion zero, which is at ~1.27 μm in the case of fused silica [16]. For the thinnest cores, the sign of the third-order dispersion coefficient β_3 ($\beta_3 = \partial^3\beta/\partial\omega^3$) changes, i.e. β_2 rises with increasing wavelength, whereas thicker cores have third-order dispersion of the same sign as that of glass and standard fibre in the wavelength range under consideration (β_2 decreases with increasing wavelength) [16]. Nonlinearity coefficients decrease almost linearly with increasing wavelength in all the cases analysed (Fig. 2, right panels). At the smallest diameter considered ($d = 1.2$ μm), the nonlinearity coefficients are the strongest functions of wavelength. At wavelengths near 2 μm, the fundamental mode is less well confined near the core in $d = 1.2$ μm fibre than in the case of thicker cores, its size is larger, and its Kerr nonlinearity coefficient is smaller.

It is often of special interest to optimise nonlinear and dispersion parameters at a wavelength near 1.55 μm, because it is close to the emission wavelength of erbium-doped fibre lasers, which can be used to pump such fibre for nonlinear optical conversion. Figure 3a shows in greater detail β_2 at a wavelength of 1.55 μm as a function of core diameter d, and Fig. 3b shows the Kerr nonlinearity coefficient γ as a function of d. Dispersion is normal at a core diameter under ~1.3 μm and anomalous for thicker cores. Note that, at a wavelength of 1.55 μm , the dispersion of standard telecom fibre SMF28e is -25 ps^2 km^{-1} and its Kerr nonlinearity coefficient is ~1 W^{-1} km^{-1}. Its material dispersion is about -28 ps^2 km^{-1}. The dispersion of SCF3, SCF4 and SCF6 at a wavelength of 1.55 μm ranges widely, from ~150 to -200 ps^2 km^{-1}, and their Kerr nonlinearity coefficients range from ~70 to ~20 W^{-1} km^{-1}. Thus, the magnitude of the dispersion of the microstructured fibres under consideration can be increased by an order of magnitude, and their nonlinearity can be increased by almost two orders of magnitude, which allows such fibre to be used in a wide range of nonlinear optical applications. Note that, with increasing core diameter d, the dispersion of SCF3, SCF4 and SCF6 approaches the material dispersion of glass (as seen in Fig. 3a, they differ little even at $d = 3$ μm). The dispersion of SCF0 asymptotically approaches the material dispersion at much larger core diameters (not shown in Fig. 3a), which is easy to account for: with increasing diameter d in SCF3, SCF4 and SCF6, the contribution of the glass walls between the air holes becomes significant, effectively increasing the cross section of the fibres relative to d. At small d, the size of the walls is considerably smaller than the wavelength, so their effect is not very strong. With increasing d, they scale linearly and have a much stronger effect.

3. Assessment of the feasibility of using suspended core fibre for producing non-classical states of light

The most widespread applications of microstructured fibre with a large Kerr nonlinearity coefficient (supercontinuum generation, soliton production including wavelength-tunable Raman solitons, four-wave interaction, and others [16]) typically take advantage of classical nonlinear-optical effects. The simulation results presented in Section 2 can be useful in designing, optimising, and implementing nonlinear optical fibre converters. At the same time, as mentioned in the Introduction section, Kerr nonlinear fibre can be used to produce non-classical states of light as well. Kerr nonlinearity is known to offer the possibility of squeezing quantum fluctuations in one of the signal quadrature components, inclined at some angle in phase space, whereas the variance of the other component increases, as shown schematically in Fig. 4, where X_1 and X_2 denote canonically conjugate field quadratures [19, 20, 22]. Such fluctuation squeezing is possible for both cw laser signals and ultrashort pulses, in particular for optical solitons [19, 20, 22]. In the case of cw signals, there is the following analytical formula for the variance of fluctuations in one of the quadratures [20]:

$$V(\theta, r_{\text{Kerr}}) = 1 + 2r_{\text{Kerr}}\sin(2\theta) + 4r_{\text{Kerr}}^2\sin^2(\theta), \qquad (4)$$

where θ is the angle of rotation in phase space; $r_{\text{Kerr}} = \gamma Pz$ is the nonlinear phase shift; z is the fibre length; and P is the signal power. The standard quantum limit corresponds to the constraint $V(\theta = 0, r_{\text{Kerr}}) = 1$. For $V < 1$, quadrature component squeezing is observed. The maximum squeezing corre-

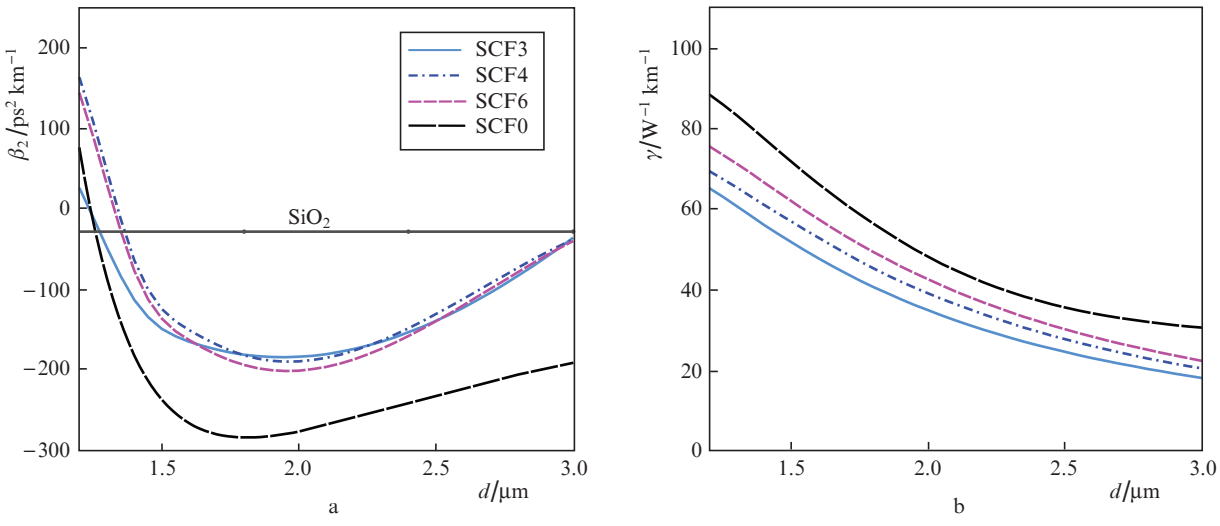

Figure 3. Calculated (a) group velocity dispersion and (b) Kerr nonlinearity coefficient at a wavelength of 1.55 μm as functions of SCF fibre diameter. The line labelled SiO_2 represents the dispersion of silica glass.

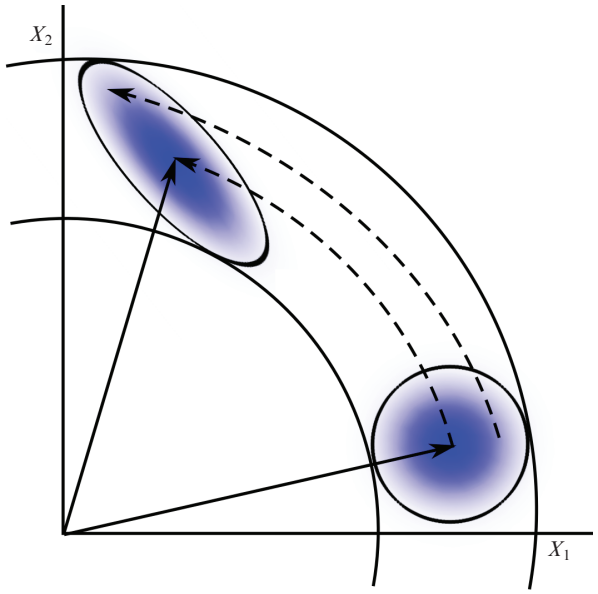

Figure 4. Schematic representation of the squeezing of fluctuations in one of the signal quadrature components in a Kerr nonlinear medium [19, 29].

sponds to the condition $(\mathrm{d}/\mathrm{d}\theta)V(\theta, r_{\mathrm{Kerr}}) = 0$, from which it follows [20] that the optimal angle of rotation is

$$\theta_{\mathrm{s}} = \frac{1}{2}\arctan\left(\frac{-1}{r_{\mathrm{Kerr}}}\right). \tag{5}$$

The largest squeezing at angle θ_{s} is given by [20]

$$V(\theta_s) = 1 - 2r_{\mathrm{Kerr}}\sqrt{1 + r_{\mathrm{Kerr}}^2} + 2r_{\mathrm{Kerr}}^2. \tag{6}$$

The degree of squeezing is often determined in experiments as $10\log_{10}V$ (dB), so it was this parameter that we calculated. Figure 5 illustrates the effect of fibre length on the optimal squeezing of quadrature component quantum fluctuations for SCF3, SCF4 and SCF6 with a core diameter of 1.2 μm, which ensures maximum nonlinearity (power $P = 10$ W). For comparison, we evaluated squeezing in a photonic crystal fibre with $\gamma = 11$ W^{-1} km^{-1} [31, 32]. It is seen that the expected squeezing in the SCFs being analyzed (above –15 dB at fibre lengths over 4 m) considerably exceeds squeezing in standard photonic crystal fibres (by more than 10 dB). At the same time, in these estimates losses are left out of account: linear absorption in the fibre (which can reach 0.078 dB m^{-1} in SCF [9]) and Fresnel reflection from the output fibre end (~0.3 dB). At a fibre length $z = 5$ m, the total loss is ~0.7 dB; at $z = 10$ m, it exceeds 1 dB, so at this level of losses the use of microstructured fibre longer than 10 m may be nonoptimal. Improving the SCF fabrication process can lead to a considerable decrease in linear optical loss, which would allow one to use longer lengths of fibre and increase noise squeezing. Besides, the use of higher power signals leads to an increase in nonlinear phase shift r_{Kerr} and, hence, to larger squeezing at the same fibre length (since losses are independent of power). The effect under discussion is also influenced by thermal noise, which was left out of consideration here and can be suppressed via cryogenic cooling. More accurate quantum fluctuation squeezing values can be obtained by simulating the stochastic generalised nonlinear Schrödinger equation [19], whereas the simple estimates made here and demonstrating the potential of SCF are useful in choosing the range of parameters and evaluating the possible squeezing limit.

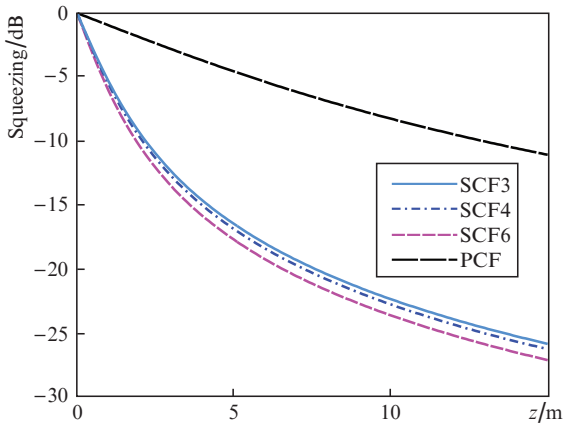

Figure 5. Effect of fibre length on quantum noise squeezing for one of the quadrature components of a 10-W cw laser signal at a wavelength of 1.55 μm, evaluated by formula (6) for SCF with $d = 1.2$ μm and photonic crystal fibre (PCF) with $\gamma = 11$ W^{-1} km^{-1}.

4. Conclusions

Dispersion and nonlinear characteristics of microstructured silica fibres with a thin suspended core surrounded by three, four or six air holes have been studied in detail in the wavelength range 1–2 μm. For comparison and verification of results, we have studied characteristics of a thin axisymmetric core in air. The number of air holes has been shown to have a rather weak effect on characteristics of the fibre (at a given core diameter). At a wavelength near 1.55 μm, corresponding to the emission wavelength of erbium-doped fibre lasers, the dispersion of the SCFs varies from ~150 to –200 ps^2 km^{-1} and their Kerr nonlinearity coefficient varies from ~70 to 20 W^{-1} km^{-1} as the SCF core diameter rises from 1.2 to 3 μm. The fabrication and use of SCF with thinner cores may be severely limited by technological and technical difficulties. The numerical simulation results obtained in this study for characteristics of SCF can be useful in designing, developing and optimising nonlinear optical fibre converters of optical signals. Moreover, we have demonstrated the feasibility and potential of using SCF exhibiting Kerr nonlinearity for generating non-classical light: a state with squeezed quantum fluctuations in one of the signal quadrature components.

Acknowledgements. This work was supported by the Russian Foundation for Basic Research (Grant Nos 19-29-11032 and 18-52-45005) and the RF Ministry of Science and Higher Education (Megagrant, Agreement No. 14.W03.31.0032).

References

1. Knight J.C., Birks T.A., Russell P.St. J., Atkin D.M. *Opt. Lett.*, **21**, 1547 (1996).
2. Zheltikov A.M. *Phys. Usp.*, **47**, 69 (2004) [*Usp. Fiz. Nauk*, **174**, 73 (2004)].
3. Dudley J.M., Genty G., Coen S. *Rev. Mod. Phys.*, **78**, 1135 (2006).
4. Litchinitser N.M., Dunn S.C., Usner B., Eggleton B.J., White T.P., McPhedran R.C., de Sterke C.M. *Opt. Express*, **11**, 1243 (2003).

5. Skryabin D.V., Luan F., Knight J.C., Russell P.S.J. *Science*, **301**, 1705 (2003).
6. Monro T.M., Ebendorff-Heidepriem H. *Annu. Rev. Mater. Res*., **36**, 46 (2006).
7. Butvina L.V., Sereda O.V., Dianov E.M., Lichkova N.V., Zagorodnev V.N. *Opt. Lett*., **32**, 334 (2007).
8. Yatsenko Y.P., Kosolapov A.F., Levchenko A.E., Semjonov S.L., Dianov E.M. *Opt. Lett*., **34**, 2581 (2009).
9. Dong L., Thomas B.K., Fu L. *Opt. Express*, **16**, 16423 (2008).
10. Hartung A., Heidt A.M., Bartelt H. *Opt. Express*, **19**, 7742 (2011).
11. Møller U., Yu Y., Kubat I., Petersen C.R., Gai X., Brilland L., Méchin D., Caillaud C., Troles J., Luther-Davies B., Bang O. *Opt. Express*, **23**, 3282 (2015).
12. El-Amraoui M., Fatome J., Jules J.C., Kibler B., Gadret G., Fortier C., Smektala F., Skripatchev I., Polacchini C.F., Messaddeq Y., Troles J., Brilland L., Szpulak M., Renversez G. *Opt. Express*, **18**, 4547 (2010).
13. Anashkina E.A., Shiryaev V.S., Koptev M.Y., Stepanov B.S., Muravyev S.V. *J. Non-Cryst. Solids*, **480**, 43 (2018).
14. Anashkina E.A., Andrianov A.V., Dorofeev V.V., Kim A.V. *Appl. Opt*., **55**, 4522 (2016).
15. Anashkina E.A., Koptev M.Y., Andrianov A.V., Dorofeev V.V., Singh S., Lovkesh, Leuchs G., Kim A.V. *J. Lightwave Technol*., **37**, 4375 (2019).
16. Agrawal G.P. *Nonlinear Fiber Optics* (San Diego: Acad. Press, 2019).
17. Finger M.A., Iskhakov T.S., Joly N.Y., Chekhova M.V., Russell P.S.J. *Phys. Rev. Lett.*, **115**, 143602 (2015).
18. Lorenz S., Silberhorn Ch., Korolkova N., Windeler R.S., Leuchs G. *Appl. Phys. B*, **73**, 855 (2001).
19. Corney J.F., Heersink J., Dong R., Josse V., Drummond P.D., Leuchs G., Andersen U.L. *Phys. Rev. A*, **78**, 023831 (2008).
20. Bachor H.A., Ralph T.C. *A Guide to Experiments in Quantum Optics* (Weinheim: Wiley-VCH, 2004).
21. Slusher R.E., Hollberg L.W., Yurke B., Mertz J.C., Valley J.F. *Phys. Rev. Lett.*, **55**, 2409 (1984).
22. Andersen U.L., Gehring T., Marquardt Ch., Leuchs G. *Phys. Scr.*, **91**, 053001 (2016).
23. Vahlbruch H., Mehmet M., Danzmann K., Schnabel R. *Phys. Rev. Lett*., **117**, 110801 (2016).
24. Milburn G.J., Levenson M.D., Shelby R.M., Perlmutter S.H., DeVoe R.G., Walls D.F. *J. Opt. Soc. Am. B*, **4**, 1476 (1987).
25. Bergman K., Haus H.A. *Opt. Lett*., **16**, 663 (1991).
26. Kitagawa M., Yamamoto Y. *Phys. Rev. A*, **34**, 3974 (1986).
27. Meissner M., Rosch M., Schmauss B., Leuchs G. *IEEE Photonics Technol. Lett*., **15**, 1297 (2003).
28. Rosenbluh M., Shelby R.M. *Phys. Rev. Lett*., **66**, 153 (1991).
29. Tran T.X., Cassemiro K.N., Söller C., Blow K.J., Biancalana F. *Phys. Rev. A*, **84**, 013824 (2011).
30. Snyder A.W., Love J.D. *Optical Waveguide Theory* (London: Chapman and Hall, 1983; Moscow: Radio i Svyaz', 1987).
31. https://www.thorlabs.com/newgrouppage9.cfm?objectgroup_id=1902.
32. https://www.nktphotonics.com/lasers-fibers/product/nonlinear-photonic-crystal-fibers/.